

## VISCOSITY AND STRUCTURAL RELAXATION OF $15\text{Na}_2\text{O}\cdot x\text{MgO}\cdot(10-x)\text{CaO}\cdot75\text{SiO}_2$ GLASSES

Mária Chromčíková\* and M. Liška

Vitrum Laugaricio (VILA) - Joint Glass Center of the Institute of Inorganic Chemistry SAS, Alexander Dubček University of Trenčín, and RONA Lednické Rovne, Študentská 2, Trenčín, 911 50, Slovak Republic

Temperature dependence of viscosity of title glasses ( $x=0, 2, 4, 6, 8, 10$ , abbreviated as M0, M2, M4, M6, M8, and M10, respectively) was measured by rotational viscometry (high temperature region:  $10^2\text{--}10^{6.5}$  dPas) and thermomechanical analysis (low temperature region:  $10^{8.5}\text{--}10^{11.5}$  dPas) and described by the Vogel–Fulcher–Tammann equation. The MgO/CaO equimolar substitution (i.e. the increasing  $x$  value) smoothly shifts the high temperature viscosity to higher values.

In the low temperature region the mixed alkali effect is demonstrated, and the highest viscosities are observed for the glasses M0 and M10. In the low temperature range the activation energy of viscous flow linearly decreases with the increasing  $x$  value ( $E_{\text{act}}/\text{kJ mol}^{-1}=479\text{--}9.0x$ ). No significant dependence of activation energy on  $x$  was found in the high temperature range ( $E_{\text{act}}/\text{kJ mol}^{-1}=238.1\pm4.2$ ). The structural relaxation was measured by thermomechanical experiment and theoretically interpreted in the frame of Tool–Narayanaswamy–Mazurin’s model. The broadening of the relaxation time spectrum was observed for the calcium-magnesium glasses in comparison with the pure calcium or magnesium glasses.

**Keywords:** glass, glass transition, relaxation phenomena, thermomechanical analysis

### Introduction

The viscosity of silicate glasses belongs to the most important properties both from the technological and theoretical point of view [1–7]. The structure relaxation as described by the Tool–Narayanaswamy–Mazurin’s (TNMa) model [8–14] is tightly bonded with the viscosity temperature dependence of both the metastable equilibrium melt and the glass with constant Tool’s fictive temperature [15, 16]. Although a large number of papers exists dealing with the temperature – composition dependence of viscosities of glass and of metastable melt, the systematic studies devoted to the compositional dependence of structural relaxation are still relatively scarce [8, 17–19]. The main effort is commonly concentrated on the methodological aspects of creating the relaxation models and the experimental work is carried out either on simple, one or two component glasses or on commercially produced glasses [17].

The present paper deals with the compositional series of sodium–magnesium–calcium silicate glasses with the constant NBO/T value (i.e. the number of non-bridging oxygens vs. tetrahedral network central atoms):

$$\text{NBO/T} = 2 \frac{2x(\text{SiO}_2) + x(\text{Na}_2\text{O}) + x(\text{MgO}) + x(\text{CaO})}{x(\text{SiO}_2)} - 4 = \\ 2 \frac{1.75}{0.75} - 4 = \frac{2}{3}$$

The magnesium free end-member is close to the common soda lime silica glass (e.g. window glass). The equimolar MgO/CaO substitution was chosen to appreciate the possible demonstration of the so-called mixed alkali effect (MAE) that manifests itself by the nonlinear compositional dependence of various properties possessing local maxima or minima [2, 20].

### Theoretical

The temperature dependence of the viscosity of glass-forming melts is described with sufficient accuracy by the empirical Vogel–Fulcher–Tammann (VFT) equation [2, 20]:

$$\log(\eta/\text{dPa.s}) = A + \frac{B}{T - T_0} \quad (1)$$

where  $T$  is thermodynamic temperature and  $A$ ,  $B$  and  $T_0$  are adjustable constants.

The viscous flow activation energy  $E_{\text{act}}$  is defined at constant pressure  $P$  by

$$E_{\text{act}} = R \left( \frac{\partial \ln \eta}{\partial 1/T} \right)_P \quad (2)$$

\* Author for correspondence: chromcikova@tnuni.sk

where  $\eta$  is the dynamic viscosity,  $T$  is the thermodynamic temperature, and  $R$  is the molar gas constant. Thus, the temperature dependent  $E_{\text{act}}$  value follows from the VFT viscosity equation:

$$E_{\text{act}} = \ln(10)RB \frac{T^2}{(T-T_0)^2} \quad (3)$$

However, in the narrow temperature range the temperature dependence of viscosity can be described with sufficient accuracy by the Arrhenius-like equation (also known as the Andrade's (AND) equation [21]):

$$\log(\eta/\text{dPas}) = A' + \frac{B'}{T} \quad (4)$$

where  $A'$ , and  $B'$  are adjustable constants.

In this case we obviously obtain the temperature independent value of activation energy of viscous flow characteristic for particular temperature-viscosity range:

$$E_{\text{act}} = \ln(10)RB' \quad (5)$$

The structural (or volume) relaxation is typically studied by dilatometry. In the present paper we use the method of thermomechanical analysis where during the zigzag time-temperature regime the length of the prismatic sample exposed to constant axial stress undergoes simultaneously the changes caused by viscous flow and by structural relaxation [22]. The method itself, as well as the optimization of the experimental schedule is discussed in our previous paper [23].

Let us consider the sample length,  $l$ , as a function of thermodynamic temperature,  $T$ , and Tool's fictive temperature  $T_f$ :

$$dl = \left( \frac{\partial l}{\partial T} \right)_{T_f} dT + \left( \frac{\partial l}{\partial T_f} \right)_T dT_f = l(\alpha_g dT + \Delta\alpha dT_f) \quad (6)$$

where

$$\Delta\alpha = \alpha_m - \alpha_g \quad (7)$$

where  $\alpha_g$  and  $\alpha_m$  is the thermal expansion coefficient of glass and of metastable equilibrium melt, respectively. The values of both thermal expansion coefficients are considered as temperature independent in the present work.

In the case when viscous flow takes place, an additional source of changes of the sample length has to be included:

$$\frac{1}{l} \left( \frac{\partial l}{\partial t} \right)_{T,T_f} = \frac{\sigma}{3\eta} \quad (8)$$

where  $\sigma$  is the axial stress,  $t$  is the time, and  $\eta$  stands for the viscosity. Let us suppose a change of the sample state from an initial state 1 to final state 2. The relative length change of the sample during the above transition, i.e. the sample strain, can be expressed as:

$$\varepsilon = \frac{l_2 - l_1}{l_1} \approx \int_{T_1}^{T_2} \alpha_g dT + \int_{T_{f,1}}^{T_{f,2}} \Delta\alpha dT_f - \left( 1 + \int_{T_1}^{T_2} \alpha_g dT + \int_{T_{f,1}}^{T_{f,2}} \Delta\alpha dT_f \right) \int_{t_1}^{t_2} \frac{\sigma}{3\eta(T, T_f)} dt \quad (9)$$

The time course of fictive temperature  $T_f$  is obtained within the frame of the Tool–Narayana–Swamy–Mazurin's model with the Kohlrausch–Williams–Watts's relaxation function [24]:

$$M(\xi) = \exp(-\xi^b) \quad 0 < b \leq 1 \quad (10)$$

where  $b$  is a constant determining the width of the spectrum of relaxation times ( $b=1$  corresponds to the single relaxation time) and  $\xi$  is the dimensionless relaxation time:

$$\xi(t) = \int_0^t \frac{dt'}{\tau(t')} = \int_0^t \frac{K}{\eta(t')} dt' \quad (11)$$

where  $\tau$  is the relaxation time. The viscosity dependence on temperature and Tool's fictive temperature can be expressed by the Mazurin's approximation:

$$\log\eta(T, T_f) = \left( A + \frac{B}{T-T_0} \right) \frac{T_f}{T} + \log\eta_0 \left( 1 - \frac{T_f}{T} \right) \quad (12)$$

The modulus  $K$  relating the viscosity and relaxation time in the Eq. (11) is considered as characteristic material constant dependent on the glass composition [25]. The VFT viscosity equation is used for the viscosity temperature dependence of metastable equilibrium melt in the Eq. (12). When the Andrade's equation is used instead of the VFT equation then  $T_0$  is set to zero and  $A$ , and  $B$  are replaced by  $A'$ , and  $B'$ , respectively.

In principle, an arbitrary subset of the above model parameters, i.e. a subset chosen from  $\{K, b, A$  or  $A', B$  or  $B', T_0, \eta_0, \alpha_g$ , and  $\alpha_m\}$ , can be estimated by means of the non-linear regression analysis. Obviously, the lower is the number of estimated parameters the more statistically robust are the results of the regression analysis. Therefore those parameters that can be estimated with sufficient accuracy by an independent experiment are not optimized in the regression analysis.

## Experimental

### Materials

Glass batches were prepared from chemically pure  $\text{Na}_2\text{CO}_3$ ,  $\text{MgCO}_3$ ,  $\text{CaCO}_3$  and  $\text{SiO}_2$ . These were

melted in a furnace at temperatures between 1773 and 1873 K in a Pt-10%Rh crucible. Homogeneity was ensured by repeated fritting and hand mixing of the glass during melting. Each melt was poured from the crucible onto a stainless steel plate. The samples were tempered in a muffle furnace for one hour at 873 K. Then the power was shut down and the samples left in the furnace until completely cool.

The chemical composition of individual samples was determined by emission spectral analysis (Na) and by complexometric titration (Ca, Mg) after the samples had been decomposed by HF and HClO<sub>4</sub> (Table 1).

### Methods

The high temperature viscosity was measured by a concentric cylinder rotation viscometer in the range of 10<sup>2</sup>–10<sup>6.5</sup> dPas using the method described by Hamlik [26]. The low temperature viscosity (10<sup>8.5</sup>–10<sup>11.5</sup> dPas) was measured by the vertical thermomechanical analyzer (Netzsch TMA 402) on prismatic samples under a constant load. The rate of axial deformation of the sample was used for the determination of viscosity (Eq (8)).

Glass transition temperature  $T_g$  was determined from the dilatometric cooling curve recorded with the cooling rate of 5 K min<sup>-1</sup> (Table 1).

The thermomechanical analyser (TMA) was used for recording the sample length during the pre-defined zigzag time-temperature schedule under the constant axial load. The time-temperature regime of the experiment started with the temperature (in K) scans 795–570–795 carried out with the heating/cooling rate of 10 K min<sup>-1</sup> followed immediately by the

scans 795–570–795 with the heating/cooling rate of 5 K min<sup>-1</sup>. In the course of the whole experiment the sample was under the constant load of 981 mN. Prismatic samples with the approximate dimensions of (5·5·20) mm<sup>3</sup> were used for the measurement. Before each experiment, the sample was heated with the rate of 5 K min<sup>-1</sup> from 290 to 820 K, and cooled down to 290 K at 5 K min<sup>-1</sup> without applied load. The non-linear regression analysis of experimental data was performed by the FORTRAN computer code based on the simplex minimization of the sum of squares of deviations, written in our laboratory.

## Results and discussion

### Chemical composition

The composition of studied samples determined by wet chemical analysis (Table 1) showed in all samples higher Na<sub>2</sub>O molar content than the required constant value of 15 mol.%. The content of the other two analyzed oxides show acceptable deviations from theoretical value in both directions. The same is true for the summary content (MgO+CaO). The significantly increased content of sodium oxide (by more than 1.5 mol.%) resulted in a slight systematic increase of the NBO/T value with respect to the theoretical value of 0.667. This obviously resulted in small decrease of viscosity and glass transition temperature, and increase of the thermal expansion coefficient.

No simple trend can be found for the  $T_g$  values shown in Table 1. The changes induced by the MgO/CaO equimolar substitution are most likely superimposed by the fluctuation of the NBO/T ratio or, more simple, of the molar content of SiO<sub>2</sub>. On the

**Table 1** Chemical composition (theor. – theoretical; anal. – obtained by chemical analysis) of studied glass samples (mol.%) and the glass transition temperature,  $T_g$

Sample	Method	Na <sub>2</sub> O	MgO	CaO	MgO+CaO	SiO <sub>2</sub> <sup>*</sup>	NBO/T	$T_g$ /K
M0	theor.	15	0	10	10	75	0.667	819
	anal.	16.54	0.00	9.92	9.92	73.54	0.720	
M2	theor.	15	2	8	10	75	0.667	797
	anal.	16.93	2.68	7.84	10.52	72.56	0.756	
M4	theor.	15	4	6	10	75	0.667	800
	anal.	17.39	4.65	5.90	10.55	72.06	0.775	
M6	theor.	15	6	4	10	75	0.667	792
	anal.	17.28	5.99	4.13	10.12	72.60	0.755	
M8	theor.	15	8	2	10	75	0.667	793
	anal.	17.64	7.05	2.22	9.27	73.10	0.736	
M10	theor.	15	10	0	10	75	0.667	794
	anal.	16.66	10.69	0.00	10.69	72.65	0.753	

\* obtained as 100–Na<sub>2</sub>O–MgO–CaO

**Table 2** The results of the regression analysis of temperature viscosity dependence; parameters of viscosity equations and their standard deviations,  $s$ ;  $s_{\text{apr}}$  – standard deviation of approximation of  $\log(\eta/\text{dPas})$ , ROT/TMA – high/low temperature range

Equation Input data	Parameter	Sample					
		M0	M2	M4	M6	M8	M10
VFT	$A$	-1.78	-2.11	-2.12	-2.06	-2.08	-2.12
	$s(A)$	0.05	0.04	0.08	0.06	0.05	0.20
	$B/\text{K}$	4 360	5 003	5 209	5 280	5 438	5 620
	$s(B)/\text{K}$	62	56	101	74	71	28
	$T_0/\text{K}$	530.3	480.6	460.2	448.2	436.7	435.1
	$s(T_0)/\text{K}$	3.6	3.2	5.7	4.2	3.9	1.5
ROT+TMA	$s_{\text{apr}}$	0.069	0.055	0.083	0.063	0.062	0.021
	$\log(\eta/\text{dPas}) \ T=850 \text{ K}$	11.9	11.4	11.2	11.1	11.1	11.4
	$\log(\eta/\text{dPas}) \ T=1550 \text{ K}$	2.50	2.57	2.66	2.73	2.80	2.92
	$A'$	-5.61	-5.40	-5.58	-5.31	-5.01	-5.02
Andrade	$s(A')$	0.16	0.13	0.17	0.14	0.09	0.07
	$B'/\text{K}$	12 589	12 367	12 753	12 448	12 124	12 330
	$s(B')/\text{K}$	213	184	226	190	116	93
ROT	$s_{\text{apr}}$	0.165	0.151	0.180	0.154	0.100	0.075
	$\log(\eta/\text{dPas}) \ T=1550 \text{ K}$	2.51	2.58	2.65	2.72	2.81	2.93
	$A'$	-18.89	-15.68	-15.88	-14.58	-13.90	-13.08
Andrade	$s(A')$	0.17	0.12	0.13	0.16	0.18	0.13
	$B'/\text{K}$	26 066	22 996	23 063	21 819	21 243	20 800
	$s(B')/\text{K}$	157	109	119	144	156	122
TMA	$s_{\text{apr}}$	0.066	0.049	0.044	0.063	0.071	0.051
	$\log(\eta/\text{dPas}) \ T=850 \text{ K}$	11.8	11.4	11.3	11.1	11.1	11.4

other hand, for the purpose of the structural relaxation experimental study these values are very important indicating the temperature where the metastable equilibrium state is reached quickly.

#### Viscosity and activation energy of viscous flow

The temperature dependence of viscosity was described by both the VFT and the Andrade (AND) equation. While the VFT equation was applied to all viscosity experimental data, the AND equation was separately applied to the low temperature viscosity values obtained by TMA analysis and to the high temperature viscosity data obtained by rotating cylinder method (ROT). The results of regression analysis are summarized in Table 2. From the low values of standard deviation of approximation it can be deduced that all the viscosity curves and their parts (i.e. low- and high-temperature) are well described by both types of viscosity equations. The viscosity values calculated for the temperature of 850 K by the VFT equation are compared with those values calculated by the AND equation in Table 2. Similarly the VFT

viscosity values are compared with the AND values calculated for the temperature of 1550 K. In both cases the agreement is at the level of experimental error of the viscosity measurement. However, lower quality of the fit can be found in the AND description of the high temperature viscosity where the standard deviation of approximation reached the values of 0.08 (M10)–0.18 (M4). Figure 1 illustrates the excellent full temperature range VFT fit for the M10 glass. On the other hand, from the course of the AND viscosity equation curves plotted in Fig. 2 can be seen that the requirement of Arrhenius-like behavior is met in both temperature regions, with the better fit observed for the low temperature viscosities. Thus, both this temperature ranges can be well characterized by the single value of activation energy of viscous flow.

From the viscosities at 1550 K (Table 2) it can be concluded that the MgO/CaO equimolar substitution (i.e. increasing  $x$  value) smoothly shifts the high temperature viscosity to higher values. Analogously, the influence of the MgO/CaO substitution on the low temperature viscosity values can be deduced from the values tabulated at 850 K. Contrary to the previous case we do

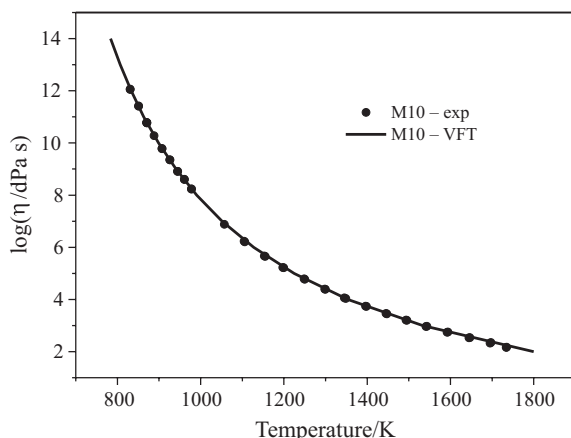


**Fig. 1** The VFT approximation (line) of the temperature viscosity dependence of the M10 glass (points – experimental viscosity values)

not observe a simple trend. The end members (M0 and M10) have the highest viscosities, but in reversed order with respect to the high temperature range. Other samples have lower (or equal – M2) viscosities without unambiguously identified trend. This can be partially rationalized by the deviations from the prescribed theoretical compositions. However, the whole set of samples indicate that the mixed alkali effect plays a decisive role in this case, i.e. the samples containing a mixture of magnesium and calcium oxides have the viscosity lower than the pure end members.

The values of activation energy of viscous flow calculated separately for the low-temperature (TMA) and high-temperature (ROT) viscosities with the use of the AND equation are summarized in Table 3. It can be seen that the  $E_{\text{act}}$  value of the high temperature part of the viscosity curve is practically independent on the MgO/CaO substitution ( $E_{\text{act}}/\text{kJ mol}^{-1}=238.1\pm 4.2$ ). The small changes observed can be attributed to variation of sodium oxide content in individual samples. It can be concluded that the activation energy of viscous flow is practically independent on the MgO/CaO equimolar substitution in the high temperature part of the viscosity curve. The dependence of the low temperature activation energy of viscous flow on the MgO/CaO substitution is visualized in Fig. 3, where  $E_{\text{act}}$  is plotted vs. the (theoretical) value

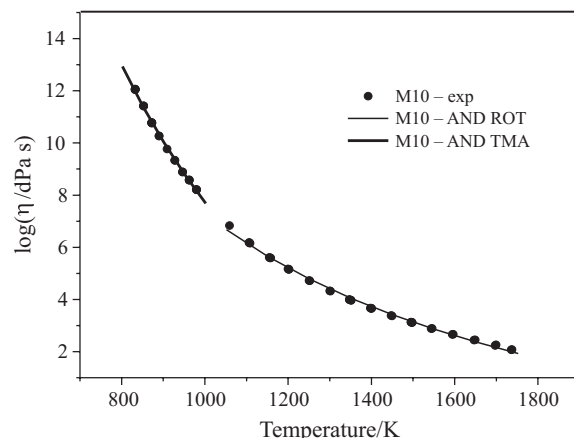


**Fig. 2** The AND approximation of the high- and low-temperature region of the temperature viscosity dependence of the M10 glass (points – experimental viscosity values)

of  $x$ . Taking into account the deviations of the chemical composition from the prescribed one it seems reasonable to consider that the plotted dependence is linear. The regression line describing the dependence with acceptable standard deviation of approximation  $s_{\text{apr}}=16 \text{ kJ mol}^{-1}$  was obtained from the regression analysis:

$$E_{\text{act}}/\text{kJ mol}^{-1} = (479 \pm 1) - (9.0 \pm 1.9)x$$

#### Structural relaxation

The results of structural relaxation study were evaluated in the frame of TNMa model with two options. First, the standard Mazurin's expression based on VFT equation was used for the dependence of viscosity on the thermodynamic temperature and on Tool's fictive temperature (Eq. (12)). Second, the AND viscosity equation obtained for the low temperature viscosity data was used instead of the VFT equation.

The thermal expansion coefficients of the glass,  $\alpha_g$ , and of the metastable melt,  $\alpha_m$ , were calculated from the first temperature derivative of the cooling dilatometric curve. The  $\alpha_g$  value was obtained from the low temperature plateau of the derivative curve, while the  $\alpha_m$  value was obtained from the maximum value reached in the high temperature part due to the

**Table 3** The values of activation energy of viscous flow,  $E_{\text{act}}$ , and their standard deviations calculated from the Andrade's viscosity equation for low- and high-temperature viscosity data (values in  $\text{kJ mol}^{-1}$ )

Input data	Parameter	Sample					
		M0	M2	M4	M6	M8	M10
High-temperature	$E_{\text{act}}$	241.04	236.78	244.18	238.34	232.14	236.07
	$s(E_{\text{act}})$	4.08	3.51	4.32	3.64	2.22	1.77
Low-temperature	$E_{\text{act}}$	499.10	440.30	441.60	417.78	406.74	398.23
	$s(E_{\text{act}})$	3.01	2.09	2.27	2.76	2.99	2.34

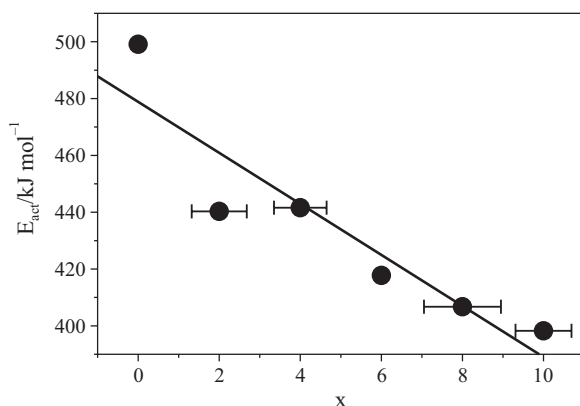


**Fig. 3** The compositional dependence of the low temperature activation energy of viscous flow. The vertical dimension of experimental points roughly corresponds to standard deviation of activation energy. The horizontal error bars reflect the difference between theoretical and analyzed MgO content

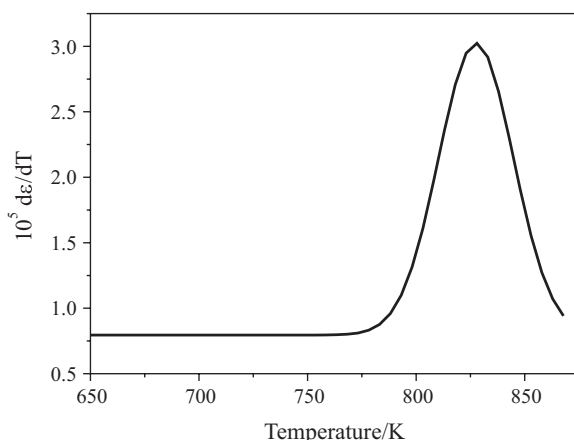


**Fig. 4** The temperature derivative of the cooling TMA curve of the M10 glass

**Table 4** The results of non-linear regression analysis of the structural relaxation experiments based on the TNMa regression model with the VFT viscosity equation. Parameter estimates are accompanied with corresponding standard deviations  $s$ ,  $s_{\text{apr}}$  – standard deviation of approximation in  $\Delta l/l_0$  units,  $F$  – Fisher's  $F$ -statistics

Parameter	M0	M2	M4	M6	M8	M10
$\log\{K/\text{dPa}\}$	10.57	10.52	10.00	8.49	9.77	10.33
$s(\log\{K/\text{dPa}\})$	0.11	0.09	0.14	0.07	0.14	0.08
$b$	0.655	0.544	0.569	0.437	0.471	0.518
$s(b)$	0.040	0.036	0.037	0.022	0.028	0.028
$\log\{\eta_0/\text{dPas}\}$	-5.43	-16.03	-0.99	5.40	-0.78	-7.90
$s(\log\{\eta_0/\text{dPas}\})$	1.72	3.37	1.47	0.53	1.13	1.92
$A$	-2.071	-2.342	-2.245	-2.317	-2.072	-2.300
$s(A)$	0.001	0.001	0.001	0.025	0.001	0.001
$F$	2 614	11 621	10 599	2 723	11 323	7 520
$10^6 s_{\text{apr}}$	149	93	125	375	112	88

**Table 5** The results of non-linear regression analysis of the structural relaxation experiments based on the TNMa regression model with the AND viscosity equation. Parameter estimates are accompanied with corresponding standard deviations  $s$ ,  $s_{\text{apr}}$  – standard deviation of approximation in  $\Delta l/l_0$  units,  $F$  – Fisher's  $F$ -statistics

Parameter	M0	M2	M4	M6	M8	M10
$\log\{K/\text{dPa}\}$	10.34	10.36	9.91	8.36	9.74	10.18
$s(\log\{K/\text{dPa}\})$	0.11	0.10	0.12	0.07	0.08	0.09
$b$	0.639	0.559	0.588	0.452	0.490	0.523
$s(b)$	0.045	0.054	0.036	0.024	0.024	0.033
$\log\{\eta_0/\text{dPas}\}$	-5.56	-22.80	-2.98	4.05	-2.73	-11.46
$s(\log\{\eta_0/\text{dPas}\})$	2.52	5.29	1.58	0.44	1.01	2.63
$A$	-19.220	-15.943	-16.037	-14.878	-13.940	-13.300
$s(A)$	0.001	0.001	0.001	0.001	0.001	0.001
$F$	2 219	8 055	9 305	2 517	9 870	5 462
$10^6 s_{\text{apr}}$	161	112	133	390	120	104

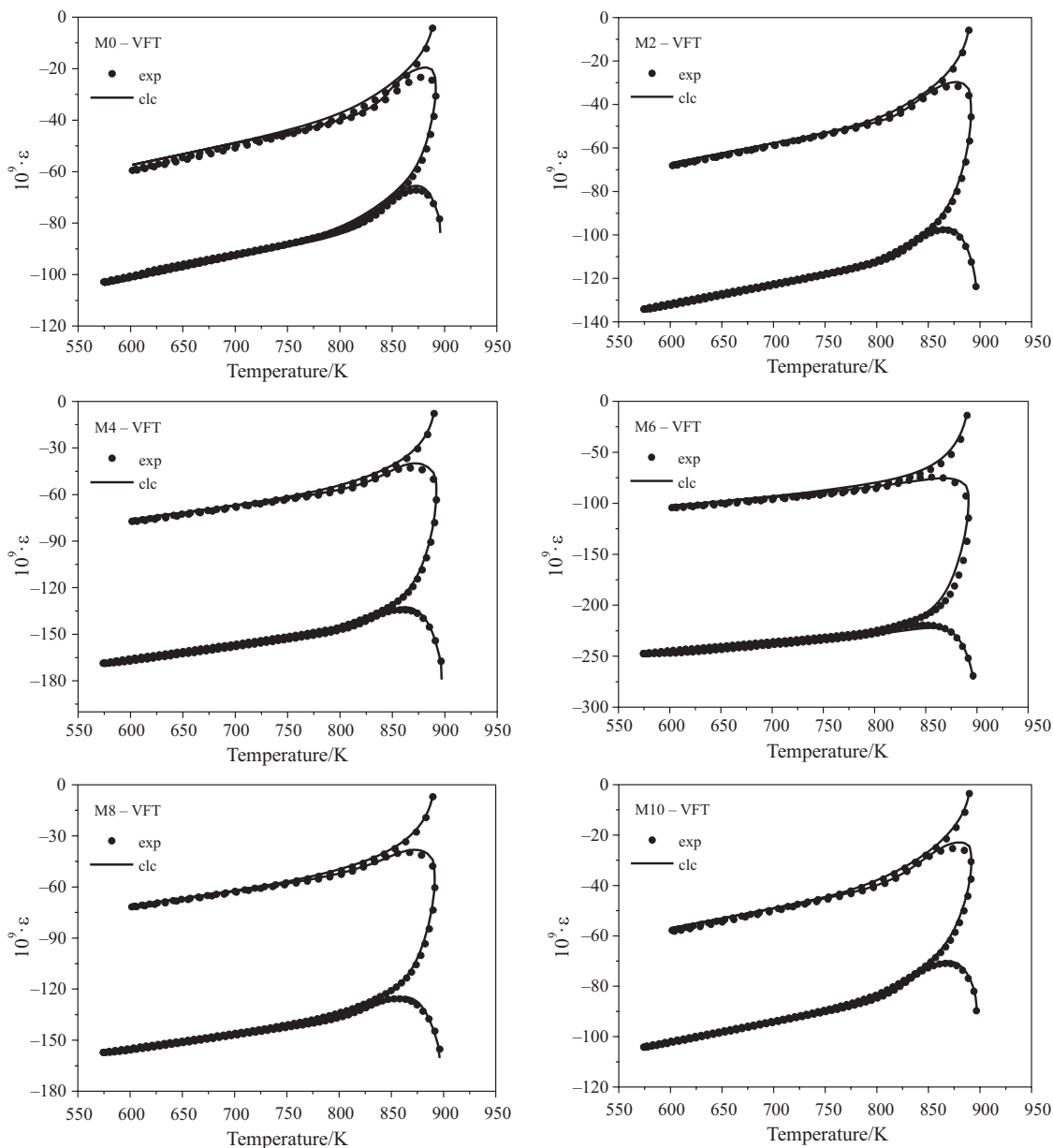


**Fig. 5** Comparison of experimental (points) and calculated (line) strain values for the TNMa–VFT model

decay of the viscous flow that was the prevailing effect at the highest temperatures (Fig. 4).

The modulus  $K$ , the KWW exponent  $b$  and the  $\log \eta_0$  were optimized with the use of a non-linear regression procedure. Due to the fact that present experimental study of viscosity reached the maximum viscosity values of  $10^{11.5}$  dPas only, and the structural relaxation experiment followed the viscous flow at even higher viscosities (close to  $10^{13}$  dPas) also the values of the  $A$  parameter of the VFT equation and the  $A'$  parameter of the AND equation were optimized. It is worth noting, that the optimization of  $A/A'$  can also formally correct the possible underestimation of the  $\alpha_m$  value that can result when the viscous flow region overlaps the transformation region, so that the maxi-

mum of the derivative curve is decreased by the viscous flow (Fig. 4).

The results of regression analysis for the VFT equation and for the AND equation are summarized in Tables 4 and 5, respectively. From the sufficiently low values of standard deviation of approximation on one side and from the relatively high values of Fisher's statistics on the other, it can be deduced that the model describes in all cases the experimental data with sufficient accuracy. This can be also deduced from the Fig. 5 (6) that graphically compares the experimental strain values with the calculated values for the VFT (AND) model.

When comparing the values of standard deviations of approximations and the values of  $F$ -statistics

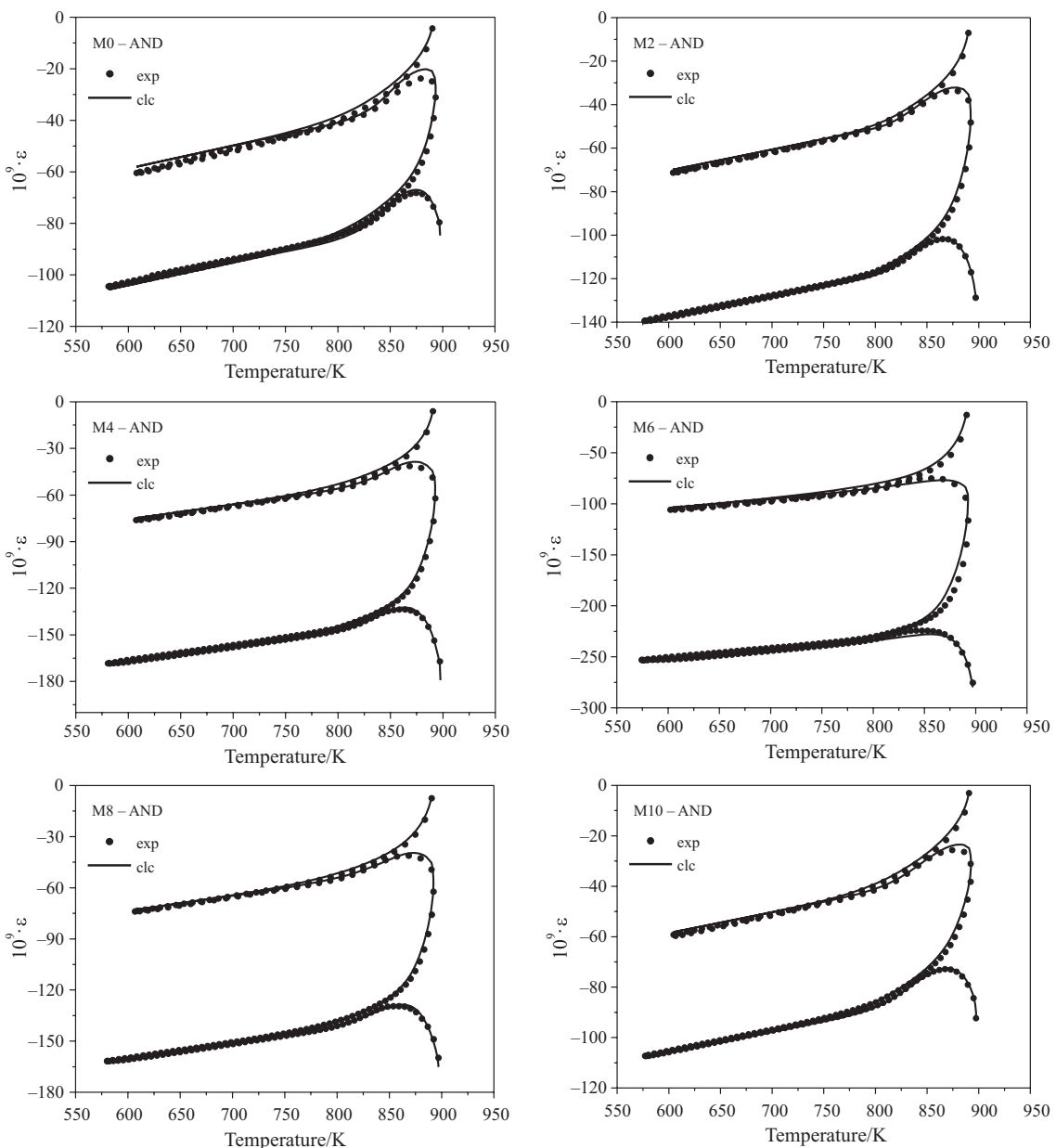


**Fig. 6** Comparison of experimental (points) and calculated (line) strain values for the TNMa-AND model

obtained for the VFT and the AND viscosity equation it can be seen that slightly better fit (i.e. lower  $s_{\text{apr}}$  and higher  $F$  values) was obtained for all studied samples in the case of the VFT equation. On the other hand, the regression estimates of the key parameters of the relaxation model, i.e.  $\log K$  and  $b$  values, are similar for both considered viscosity equations. The estimates of  $\log(\eta_0)$  are obtained with relatively high standard deviations indicating that the particular values have in some cases negligible statistical significance. This is in accord with the high dispersion of the  $\log(\eta_0)$  values obtained within the set of studied glasses, some of them being physically unacceptable (e.g. for M2, M6, and M10 glass). Having in mind

that the  $\log(\eta_0)$  value describes the temperature dependence of the iso-structural glass viscosity that is typically higher than  $10^{13}$  dPas we can deduce, that this effect is in the present experimental design superimposed both by the viscous flow at lower viscosities and by the structural relaxation process, which takes place in the glass transition region. Simply speaking, we have not collected enough experimental data to describe the glass viscosity at constant Tool's fictive temperature with sufficient accuracy.

The  $b$  parameter of the KWW Eq. (10) reflects the width of the spectrum of relaxation times. It can be seen that the narrowest distribution, i.e. the highest  $b$  value, is obtained for the pure calcium glass (M0).

The broadest distribution is observed for the mixed magnesium-calcium glasses M6 and M8. This can be rationalized by the structural disorder increasing with the increasing field strength of the M<sup>2+</sup> ion on one side and by the disorder caused by the Ca<sup>2+</sup>-Mg<sup>2+</sup> mixing in the glass structure on the other. Due to the higher field strength of Mg<sup>2+</sup> the Q-speciation of the pure magnesium glass M10 is broader with respect to the pure calcium glass M0 [27]. Then the lower value of *b*, i.e. the broader distribution of relaxation times, can be explained by the more disordered structure in which greater diversity of relaxation mechanisms is present. The regression estimates of the log*K* values obey similar dependence on the MgO/CaO substitution like the *b* values.

## Conclusions

The MgO/CaO equimolar substitution smoothly shifts the high temperature viscosity to higher values. In the low temperature region the mixed alkali effect is demonstrated, and the highest viscosities are observed for M0 and M10 glasses. In the low temperature range the activation energy of viscous flow decreases almost linearly with the increasing *x* value (*E*<sub>act</sub>/kJ mol<sup>-1</sup>=479–9.0*x*). No significant dependence of activation energy on *x* was found in the high temperature range (*E*<sub>act</sub>/kJ mol<sup>-1</sup>=238.1±4.2).

The structural relaxation is well described by the Tool–Narayanaswamy–Mazurin’s model based on the Vogel–Fulcher–Tammann viscosity equation. Similar results are obtained by the model based on the Andrade’s viscosity equation parameterized on the low temperature viscosity experimental values measured by thermomechanical analysis.

The narrowest distribution of structural relaxation times was obtained for the pure calcium glass M0. The broadest distribution was observed for the mixed magnesium-calcium glasses M6 and M8. The broader distribution of relaxation times can be explained by a more disordered structure with larger diversity of relaxation mechanisms.

## Acknowledgements

This work was supported by Agency for Promotion Research and Development under the contract No. APVV-20-P06405, and by the Slovak Grant Agency for Science under the grant No. VEGA 1/3578/06.

## References

- O. V. Mazurin, Ju. K. Starcev and R. Ja. Chodakovskaja, Relaxacionnaja teorija otzhiga stekla i raschet na jej osnove rezhimov otzhiga (in Russian), Moskovskij Chimikotechnologicheskij Institut, Moskva 1986.
- K. J. Rao, Structural Chemistry of Glasses,.. Elsevier, Amsterdam 2002.
- H. Scholze and N. J. Kreidl, Technological Aspects of Viscosity, pp. 233–273 In: Viscosity and Relaxation, (Eds. D. R. Uhlmann and N. J. Kreidl), Glass: Science and Technology, Vol. 3, Acad. Press, New York 1986.
- J. Hadac, P. Slobodian and P. Saha, *J. Therm. Anal. Cal.*, 80 (2005) 81.
- P. Pustkova, J. Shanelova, J. Malek and P. Ciezmanec, *J. Therm. Anal. Cal.*, 80 (2005) 643.
- M. Liska and M. Chromcikova, *J. Therm. Anal. Cal.*, 81 (2005) 125.
- M. Chromcikova and M. Liska, *J. Therm. Anal. Cal.*, 84 (2006) 703.
- C. A. Angell, K. L. Ngai, G. B. McKenna, P. F. McMillan and S. W. Martin, *J. Appl. Phys.*, 88 (2000) 3113.
- G. W. Scherer, Relaxation in Glass and Composites, J. Wiley&Sons, New York 1986.
- G. W. Scherer, *J. Am. Ceram. Soc.*, 69 (1986) 374.
- O. S. Narayanaswamy, *J. Am. Ceram. Soc.*, 54 (1971) 491.
- O. V. Mazurin, Relaxation Phenomena in Glass, In: Proc. XI. Int. Congr. Glass, pp. 130–169, ČSVTS-DT, Prague 1977.
- O. V. Mazurin, Steklovanie (in Russian), Nauka, Leningrad 1986.
- I. Gutzow, Ts. Grigorova, I. Avramov and J. W. P. Schmelzer, *Phys. Chem. Glasses*, 43C (2002) 477.
- A. Q. Tool, *J. Res. Natl. Bur. Stand.*, 34 (1945) 199.
- A. Q. Tool, *J. Am. Ceram. Soc.*, 29 (1946) 240.
- U. Hotheringham, Chap. 4.1. In: Analysis of the Composition and Structure of Glass and Glass Ceramics, H. Bach and D. Krause Editors, Springer, Berlin 1999.
- L. D. Pye, A. Montenero and I. Josephs (Editors), Properties of Glass-Forming Melts, CRC Press, Boca Raton 2005.
- T. P. Seward III and T. Vascott, High Temperature Glass Melt Property Database for Process Modeling, Am. Ceram. Soc., Westerville, OH 2005.
- W. Vogel, Glass Chemistry, Springer, Berlin 1992.
- E. N. Andrade, *Philos. Mag.*, 17 (1934) 497; 17 (1934) 698.
- M. Liška, I. Štubňa, J. Antalík and P. Perichta, *Ceramics*, 40 (1996) 15.
- M. Chromčíková and P. Dej, *Ceramics*, 50 (2006) 139.
- G. Williams, D. C. Watts, B. S. Dev and A. N. North, *Trans. Faraday Soc.*, 67 (1971) 1323.
- I. M. Hodge, *J. Res. Natl. Inst. Stand. Technol.*, 102 (1997) 195.
- L. Hamšík, Sklář a keramik, 31 (1987) 43.
- B. O. Mysen, Structure and Properties of Silicate Melts, Elsevier, Amsterdam 1988.

Received: October 16, 2006

Accepted: October 19, 2006

OnlineFirst: February 26, 2007

DOI: 10.1007/s10973-006-7976-5